

**Supporting Information for**

**Intersectin deficiency impairs cortico-striatal neurotransmission and causes obsessive-compulsive behaviors in mice**

Dennis Vollweiter, Jasmeet Kaur Shergill, Alexandra Hilse, Gaga Kochlamazashvili, Stefan Paul Koch, Susanne Mueller, Philipp Boehm-Sturm, Volker Haucke, Tanja Maritzen

Corresponding authors: Volker Haucke and Tanja Maritzen

Email: haucke@fmp-berlin.de and maritzen@rptu.de

**This PDF file includes:**

Supporting Text: Extended Methods  
Figures S1 to S5  
Tables S1 to S6  
Legend for Movie S1  
SI References

**Other supporting materials for this manuscript include the following:**

Movie S1: Obsessive corner jumping by ITSN dKO mice

## **Supporting Text: Extended Methods**

### **Animals**

ITSN dKO mice were generated by crossing ITSN1 KO and ITSN2 KO mice (1, 2). After establishing that ITSN2 KO mice do not show any behavioral abnormalities and thus can be used as controls, ITSN dKO mice were generated by crossing ITSN1<sup>+/-</sup>/ITSN2<sup>-/-</sup> mice to increase the number of ITSN dKO mice obtainable per breeding in line with the 3R principles. Animals were group-housed under a 12 h light/dark cycle with food and water ad libitum. All experiments in the present study were conducted in accordance with the guidelines of the LAGeSo Berlin and with their permission. Intersectin dKO mice were bred under the licenses G0357/13 and G0153/19, and additional behavior experiments were performed under license G0144/17.

### **Mouse observation in home cage environment**

Adult ITSN2 KO and dKO mice of both sexes were individually observed for 10 min in a typical home cage environment (23x36 cm plastic cage with a several cm high layer of bedding, one paper towel, metal lid). Movies were manually scored for the occurrence of diverse behaviors by an experimenter blinded to genotype.

### **Nesting**

A single fresh paper towel was placed into a home cage housing a single mouse. After 24 h the quality of the formed nest was scored with 0 meaning that the paper was unaltered, 1 indicating that the paper was partially unfolded, 2-4 indicating that the paper had been increasingly remodeled into a nest.

### **Marble assay**

A typical home cage was filled 5 cm high with bedding, and 20 black marbles of 16 mm diameter were placed in 5 equally spaced rows à 4 marbles, and a picture was taken. Mice were singly placed in the upper left corner of the cage facing towards the wall. After 30 min the mouse was gently removed from the cage, and a picture was taken again. Based on the before/after pictures it was manually counted how many marbles had been displaced by the mouse. In addition, the software Fiji was used to determine the visible area of the marbles on the before/after pictures to calculate the % bead area covered by bedding after the mouse had been taken out of the cage.

### **Infrared light-beam activity monitoring**

To quantitatively assess movement of ITSN2 KO and dKO mice, we compared 30 age- and sex-balanced adult animals per genotype. For activity tests individual mice were transferred into a fresh home cage (23x36 cm) including new bedding. Water (in a flat petri dish), gelatine and food pellets were provided in the center of the cage to not interfere with infrared beams. Activity measurements were performed for 24 h using the PhenoMaster ActiMot2 module providing infrared beams in xyz to record horizontal movement and jumping.

The collected activity data was also used to analyze sleeping patterns. Based on (3) any episode of continuous inactivity of  $\geq 40$  s was considered to be sleep. Activity was determined within 10-s epochs.

### **Fluoxetine treatment**

Fluoxetine was dissolved in water and administered at a dose of 18 mg/kg per day in the drinking water for 3 weeks.

### **Elevated plus maze**

The mice were placed at the center of the elevated plus maze (Ugo Basile #40143 Elevated Plus Maze Mouse) facing a closed arm. Their behaviour was recorded for 5 min. To be counted as an entry the mouse had to enter an arm with all four paws.

### **Beam walking test**

A ~40 cm long round beam made from glass was placed in a way that each end connected to the top of a standard home cage i.e. ~15 cm above the ground. Underneath the beam paper towels

were placed to cushion any potential falls. For each of the six consecutive trials the respective ~2-months-old mouse was placed gently onto the middle of the beam. The run was finished when the mouse reached the home cage at either end or fell off the beam. Performance was graded in the following manner with the results of all trials being averaged: A score of 2 was assigned when the mouse successfully crossed the beam and entered a cage. A score of 1 was assigned when the mouse was able to stay on the beam for some time before falling off. A score of 0 was assigned when the mouse was not able to grip or stay on the beam at all and fell off immediately upon placement.

### **Magnetic resonance imaging (MRI)**

MRI was performed on n=9 age-matched ITSN2 KO and dKO mice using a 7 Tesla rodent scanner (BioSpec, Bruker, Ettlingen, Germany) equipped with Paravision 6.0.1 software and a <sup>1</sup>H-Cryoprobe. During the examination the animal was placed on a heated circulating water blanket to ensure a constant body temperature of 37°C. Anaesthesia was induced with 2.5% and maintained with 2.0-1.5% isoflurane delivered in a O<sub>2</sub>/N<sub>2</sub>O mixture (0.3/0.7 L/min) via a facemask under constant respiration rate monitoring using a pressure sensitive pad placed on the thorax. For anatomical imaging a high resolution T2-weighted turbo spin-echo sequence was used (2D RARE, repetition time (TR)=4250 ms, echo time (TE)=33 ms, RARE factor=8, 2 averages, 40 axial slices, slice thickness=0.40 mm, field of view (FOV)=19.2x19.2 mm<sup>2</sup>, matrix size=192x192, readout bandwidth (BW)=34.7 kHz, scan time 3:24 min). For measuring the volumes of different brain structures, the Allen Brain Atlas (<https://mouse.brain-map.org/>) was registered to the anatomical images in ANTx2 (<https://github.com/ChariteExpMri/antx2>)(4). Further statistical analysis of volumetric changes between genotypes was performed using R statistical programming language. Volumetric data of brain subregions was expressed both as absolute volume (mm<sup>3</sup>) and relative volume (absolute subregion volume/total brain volume\*100%). Average brain region volume and variance was calculated for each region of the annotation ontology, and relative changes of volume between genotypes were expressed as  $(Vol^{dKO}-Vol^{2KO})/Vol^{2KO}*100\%$  allowing to rank brain regions by relative magnitude of volume reduction. Additionally, differences in brain region volumes were compared for statistical significance by applying unpaired t-tests, which were corrected for multiple comparisons by the false-discovery rate (FDR) approach of Benjamin-Hochberg as implemented in the “adjust\_pvalue” method from the rstatix package 0.7.0 in the R programming language.

DTI was performed using a spin-echo Stejskal Tanner sequence with geometry matching the anatomical imaging (2D SE-EPI, 5 b=0 images, 60 directions with b=1000 s/mm<sup>2</sup>, TR=3500 ms, TE=30 ms, matrix size 160x160, BW=300 kHz, scan time 15:10 min). DTI maps were generated in DSI Studio (<https://dsi-studio.labsolver.org/>). Voxel-based independent t-statistics for DTI-maps of fractional anisotropy and axial/radial/mean diffusivity (FA, AD, RD, MD) were calculated in Allen mouse brain space using SPM-12 (<https://www.fil.ion.ucl.ac.uk/spm/software/spm12/>).

### **Acute brain slice preparation**

Acute coronal slices were prepared from 3-5 weeks (patch clamp) and 9-12 weeks (field recordings) old ITSN2 KO and dKO mice. Mice were killed by cervical dislocation, and brains were rapidly dissected and placed into ice-cold carbogenated (95% O<sub>2</sub>, 5% CO<sub>2</sub>) cutting solution (135 mM NMDG, 1 mM KCl, 1.2 mM KH<sub>2</sub>PO<sub>4</sub>, 10 mM glucose, 20 mM choline bicarbonate, 1.5 mM MgSO<sub>4</sub>\*7H<sub>2</sub>O, 0.5 mM CaCl<sub>2</sub>\*2H<sub>2</sub>O; pH 7.45; 305-310 mOsm/kg). After removing the cerebellum, brains were glued to the vibratome holder plate using tissue adhesive and structurally supported by additionally glueing a small agarose block (2% agarose in H<sub>2</sub>O) dorsally of the brain. Hemispheres were separated by a medial cut through the midline along the rostrocaudal axis. Subsequently, 300 μm thick coronal slices containing dorsolateral striatum were prepared in ice-cold carbogenated cutting solution using a vibratome (Leica, VT 1200S) and transferred to a self-made incubation chamber at 35°C with carbogenated artificial cerebrospinal fluid (aCSF: 119 mM NaCl, 2.5 mM KCl, 1 mM NaH<sub>2</sub>PO<sub>4</sub>, 26 mM NaHCO<sub>3</sub>, 20 mM glucose, 1.3 mM MgCl<sub>2</sub>\*6H<sub>2</sub>O, 2.5 mM CaCl<sub>2</sub>\*2H<sub>2</sub>O; pH 7.35; 305-310 mOsm/kg), which was also used for recording. After 15 min the incubation chamber was removed from the heated bath, and slices were allowed to recover for at least another 60 min at room temperature before experiments.

### **Striatal field recordings**

For extracellular field recordings a coronal slice was placed in a recording chamber and fixed with a nylon mesh and two custom-made steel anchors to hold the slice in place during recordings. The recording chamber was mounted on a stable platform serving as the specimen stage of an upright BX-61WI brightfield microscope (Olympus). During recordings the brain tissue was constantly perfused with carbogenated aCSF at 30°C at a rate of approximately 2 ml/min using gravity flow and a peristaltic pump (ISMATEC), and an in-line heater that was controlled with Lin-Lab Software (Scientifica). An EPC9 patch-clamp amplifier together with an ITC-16 analog-to-digital converter were used to acquire electrical recordings (Heka Electronics). Signals were sampled at 20 kHz and filtered at 5 kHz (Bessel filter) using PATCHMASTER software (Heka Electronics). Glutamatergic corticostriatal transmission was pharmacologically isolated by supplementing the recording aCSF with 20  $\mu$ M (–)-Bicuculline methiodide, a GABA<sub>A</sub> receptor antagonist, and 50  $\mu$ M AP-5, an NMDA receptor antagonist, to prevent unwanted downstream plasticity. Responses were evoked after placing the stimulating electrode (WE5ST30.5B10, MicroProbes, Gaithersburg, MD, USA) at the inner edge of corpus callosum within the dorsolateral striatum. Borosilicate glass pipettes (7740 Glass, ID 1, OD, 1.5, Length 100, King Precision Glass, Inc., Claremont, CA, USA) were pulled using a P-1000 horizontal electrode puller (Sutter Instruments), backfilled with recording aCSF to yield a tip resistance of ~2 M $\Omega$  and used to record extracellular field responses in the dorsolateral striatum approximately 400–450  $\mu$ m away from the stimulating electrode.

Input-output curves were generated by successively stimulating slices with a biphasic 200  $\mu$ s current pulse at increasing stimulation intensities and recording the corresponding compound presynaptic action potentials (also called fiber volleys, FV) and postsynaptic ensemble somatodendritic depolarizations (population spikes, PS). To reduce the impact of electrical noise and variability of responses, for each current intensity, responses were evoked three times and averaged with 20 s inter-stimulation interval to prevent plasticity induction. Generally, the amplitude of the PS was measured by first constructing a helper line connecting the left and right positivity of the PS. The length of the vertical projection from the helper line to the PS minimum was taken as the amplitude of the PS. Similarly, the amplitude of the FV was taken as the length of the vertical projection from the FV minimum to the subsequent left positivity of the PS.

To analyze corticostriatal long-term depression of striatal field responses, cortical afferents were stimulated every 20 s for 10 min to determine baseline neurotransmission with a stimulation intensity that evokes ~50-60% of maximal PS amplitude. High-frequency stimulation-induced long-term depression was triggered by delivering 100 Hz stimulation trains for 1 s (four times, 10 s inter-train interval) at a stimulation intensity that evoked maximum PS amplitude. Depression of striatal responses was recorded by probing PSs every 20 s for an additional 40 min with the same stimulus intensity as used for initial base-line recording. To reduce variability of PS amplitudes, response curves were smoothed by plotting the average of six sampled points resulting in average data points for 2 min intervals.

### **Striatal patch clamp recordings**

All recordings were performed at 30°C as described for extracellular recordings. Medium spiny neurons in the dorsolateral striatum were identified by shape and size (ovoid cell body with major axis of 10-14  $\mu$ m) using infrared-differential interference contrast (IR-DIC) visualization. Interneurons if identified by high spontaneous activity and large series resistance (cut-off value 40 M $\Omega$ ) were discarded from analysis. Criteria for acceptance were uncompensated stable access resistance < 25 M $\Omega$  and holding current < -300 pA. Recording patch pipettes yielded a tip resistance of 2.5–4.5 M $\Omega$ , when filled with the internal solution (107 mM CsMeSO<sub>3</sub>, 10 mM CsCl, 3.7 mM NaCl, 5 mM TEA-Cl, 20 mM HEPES, 0.2 mM EGTA, 5 mM Lidocaine N-ethyl chloride, 4 mM ATP-Mg, 0.3 mM GTP-Na<sub>3</sub>, pH 7.3, 300 mOsm/kg), which was kept on ice during the whole experiment. For measuring the ratio of NMDAR- to AMPAR-mediated synaptic currents, inhibitory GABA<sub>A</sub> receptor-mediated transmission was blocked using 20  $\mu$ M (–)-Bicuculline methiodide supplemented in the recording aCSF. Excitatory postsynaptic currents (EPSCs) were locally evoked using a stimulating electrode placed at the inner edge of corpus callosum within the dorsolateral striatum as described for extracellular recordings, while holding the cell at potentials of -80 mV and +40 mV, respectively. At -80 mV membrane potential NMDARs are blocked by Mg<sup>2+</sup> ions and neurotransmission is mediated by AMPARs, while at +40 mV NMDARs are

unblocked and contribute to current flow across the postsynaptic membrane. The stimulus intensity was set at a level that evoked 100-300 pA AMPAR-mediated EPSCs measured at -80 mV. Evoked responses were averaged 10x with an inter-stimulus interval of 20 s. The peak negative current at -80 mV was considered to be fully mediated by AMPARs and defined as the AMPAR current. The NMDAR current measured at +40 mV was defined as the average positive current response within a 2.5 ms measurement window beginning 50 ms after current onset, where AMPAR-mediated current kinetics have decayed substantially. The NMDAR/AMPA current ratio was obtained by dividing the respective current values.

To characterize spontaneous release of neurotransmitter-filled vesicles, spontaneous excitatory postsynaptic currents (sEPSCs) were recorded. To this end, cells were voltage-clamped at -80 mV in the presence of 20  $\mu$ M (-)-Bicuculline methiodide and 50  $\mu$ M AP-5. Spontaneous transmission was not recorded until 3 min after entering whole-cell configuration to allow the dialysis of Cs<sup>+</sup> internal solution for a relatively complete block of the potassium channels in the medium spiny neurons. Subsequently, spontaneous neurotransmission was acquired for 45 sweeps of 5 s length and the series resistance probed at the end of each sweep by applying a 5 mV test pulse for 20 ms. Sweeps were rejected from analysis if series resistance changed by more than 20% or holding current exceeded 400 pA. Analysis of sEPSCs was performed using Mini Analysis software after application of a digital 1 kHz elliptic low-pass filter to reduce electrical noise and setting a threshold of 5 pA to detect spontaneous release events. At least 3 min of spontaneous activity were assessed for each cell, and average amplitude and frequency were used for statistical analysis.

### **Staining and morphological analysis of medium spiny neurons**

Medium spiny neurons were filled with neurobiotin during patch clamp experiments. Internal solution was supplemented with 0.2% (w/v) neurobiotin, and after recordings the electrode was gently removed from the patched neuron to promote resealing of the somatic membrane and avoid leakage of neurobiotin. After 1-2 min of resting in the recording solution to wash away residual neurobiotin, slices were fixed with 4% (w/v) paraformaldehyde in 0.1 M phosphate buffer (PB) pH 7.4 at 4°C overnight. Afterwards, the fixative was removed, and slices were washed 3x in 0.1 M PB for 5 min each. Subsequently, slices were blocked and permeabilized in blocking solution (10% (v/v) normal goat serum, 0.3% (v/v) Triton-X 100, 0.1 M PB) for 1 h at room temperature and subsequently stained with 1:400 Streptavidin Alexa Fluor™ 594 conjugate in staining solution (50% (v/v) blocking solution, 50% (v/v) 0.1 M PB) for 2 days at 4°C on a shaker. After washing 3x 10 min in 0.1 M PB slices were mounted on Superfrost microscopy slides using ProlongGold Antifade mounting medium. After 48 h neurobiotin-filled medium spiny neurons were imaged using an LSM710 laser-scanning microscope, equipped with a 40x objective, a T-PMT light detector, and an HXP 120 C light unit together with an Ar-Ion laser. Fluorescence was excited at 561 nm. The signal was acquired in 3x3 tiled image acquisition mode and as z-stacks with a distance of 0.4  $\mu$ m.

To assess dendritic complexity, Sholl analysis was performed using Fiji and the 'Sholl Analysis' plugin. First, the Streptavidin-AlexaFluor594-stained medium spiny neuron was thresholded and outlined as a binary mask, then concentric rings with a distance of 10  $\mu$ m from the soma were used to calculate intersections with the dendritic tree at a distance of 15  $\mu$ m to 195  $\mu$ m from the cell body.

To determine the density of dendritic spines, their number was counted on a dendritic branch approximately 20  $\mu$ m in length using the multi-point tool implemented in Fiji and then divided by the length of the branch. For each neuron this was repeated for two different segments of the dendritic branch. The results were averaged to account for variability in spine density across a given neuron.

### **Preparation of neuronal cell cultures for STED imaging**

Hippocampal neurons were isolated from postnatal day 0-3 mouse brains. Hippocampi were dissected, placed into ice-cold HEPES-buffered Hank's balanced salt solution (HBSS, Thermo Fisher Scientific) containing 20% fetal bovine serum (FBS), and cut with a scalpel into ca. 1 mm<sup>3</sup> sized pieces. The tissue pieces were washed with HBSS containing 20% FBS and then with HBSS and afterwards were digested for 15 min in digestion buffer (137 mM NaCl, 5 mM KCl, 7 mM Na<sub>2</sub>HPO<sub>4</sub>, 25 mM HEPES, 1 mg/ml trypsin, 1500 units DNase, pH 7.2) at 37°C, followed by another

washing step with HBSS and gentle trituration in dissociation buffer (HBSS containing 12 mM MgSO<sub>4</sub>, 1500 units DNase, pH 7.2). 50,000 hippocampal neurons were plated as 20 µl drops per poly-L-lysine-coated coverslip within a 12-well plate. 1 ml of plating medium (MEM supplemented with 0.5% glucose, 0.02% NaHCO<sub>3</sub>, 0.01% transferrin, 10% FBS, 2 mM L-glutamine, 25 µg/ml insulin and 1% penicillin/streptomycin) was added per well 1 h after plating. After one day in vitro (DIV1), half of the plating medium was replaced by growth medium (MEM containing 5% FBS, 0.5 mM L-glutamine, 1x B27 supplement, 1% penicillin/streptomycin). On DIV2, 500 µl of growth medium was added per well. 2 µM AraC were used during medium renewal to limit glial proliferation. Neurons were maintained at 37°C in a 5% CO<sub>2</sub> humidified incubator until DIV14-16.

#### **Time-gated STED imaging of neurons**

On DIV14-16, neurons were fixed using ice-cold methanol fixation solution [for 100 ml: 90 ml methanol and 10 ml MES-based solution (100 mM MES, 1 mM EGTA, 1 mM MgCl<sub>2</sub>, pH 6.9)] for 5 min at -20°C and blocked with 1% BSA and 3% normal goat serum in PBS for 30 min. Neurons were then incubated with primary antibodies diluted in 1% BSA and 3% normal goat serum in PBS overnight at 4°C, followed by appropriate secondary antibodies diluted 1:400 in PBS for 1 h at room temperature. Coverslips were mounted using Prolong Gold Antifade (Invitrogen, #P36930) and stored at 4°C until imaging. STED imaging with time-gated detection was performed on a Leica SP8 TCS STED microscope (Leica Microsystems) equipped with a pulsed white-light excitation laser (WLL; ≈80 ps pulse width, 80 MHz repetition rate; NKT Photonics) and one STED laser for depletion at 775 nm. The pulsed 775 nm STED laser was triggered by the WLL. Three-channel STED imaging was performed by sequentially exciting ATTO542, Alexa594, and ATTO647N at 539 nm, 594 nm, and 646 nm, respectively. Time-gated detection was set from 0.5–6 ns for all dyes. Fluorescence signals were detected sequentially by hybrid detectors at appropriate spectral regions distinct from the STED laser. Images were acquired with an HC PL APO CS2 100x/1.40 N.A. oil objective (Leica Microsystems), a scanning format of 1024x1024 pixels, eight-bit sampling, and 6x zoom, yielding a pixel dimension of 18.94x18.94 nm.

#### **Preparation of synaptic P3 fraction from mouse brain**

Dissected forebrains were homogenized in 8 ml ice-cold homogenization buffer (4 mM HEPES pH 7.4, 320 mM sucrose, 1 mM PMSF, 1x cComplete EDTA-free protease inhibitor cocktail (Sigma-Aldrich)) with 12 homogenizer strokes at 1000 rpm. Large debris and nuclei were sedimented at 1000xg for 10 min at 4°C, and the pellet (P1) was discarded. The supernatant S1 was centrifuged at 12500xg for 15 min at 4°C to retrieve the crude synaptosomal fraction P2, and the supernatant S2 was discarded. The pellet P2 was resuspended in ice-cold homogenization buffer and centrifuged at 12500xg for 15 min at 4°C, discarding the supernatant S2' and keeping the crude washed synaptosomal fraction P2'. P2' was resuspended in 2 ml ice-cold H<sub>2</sub>O for hypotonic lysis. The resuspended synaptosomes diluted with another 6 ml of H<sub>2</sub>O were homogenized with three slow strokes at 300 rpm. To stabilize pH, an appropriate amount (~30 µl) of 1 M HEPES pH 7.4 was added to the samples to achieve 4 mM final concentration. Samples were rotated for 30 min at 4°C for complete lysis. Lysed membranes were centrifuged at 25000xg for 30 min at 4°C to pellet the lysed synaptosomal membrane fraction P3. Each pellet was resuspended in the same volume of 650 µl 2x SDS sample buffer (20% (v/v) glycerol, 120 mM Tris/HCl pH 6.8, 4% (w/v) SDS, 0.02% (w/v) bromphenol blue, 5% (v/v) β-mercaptoethanol) and left to dissolve for 20 min at RT. Samples were boiled at 95°C for 10 min and analyzed by immunoblotting.

#### **Trypsin cleavage assay**

Synaptosomes were isolated similarly to above. The entire mouse brain was homogenized with 12 strokes at 900 rpm in 8 ml ice-cold homogenization buffer (320 mM sucrose, 5 mM HEPES, pH 8) before centrifuging at 900xg for 10 min at 4°C. The supernatant (S1) was centrifuged at 10,000g for 15 min at 4°C yielding the synaptosomal pellet (P2). P2 was resuspended in 2 ml of ice-cold sucrose buffer, diluted with 6 ml homogenization buffer and centrifuged at 15,000g for 15 min at 4°C. The washed synaptosomal pellet was resuspended in 2 ml homogenization buffer. The protein concentration was measured using Bradford assay. For the tryptic cleavage of synaptosomes, a trypsin (Sigma #59427C) stock solution of 0.1 mg/ml was prepared, and different trypsin amounts (12.5 µg, 25 µg, 50 µg, 125 µg) were added to 3-5 mg of synaptosomal lysates. The mixtures were

incubated for 10 min at 30°C with gentle agitation, followed by centrifugation at 8700xg for 3 min at 4°C. The resulting pellet was resuspended in 1x Laemmli buffer and boiled at 93°C for 10 min. The samples were analyzed by immunoblotting. Imaging was done using the Image Studio software package of the Odyssey Fc Imaging System (LI-COR Biosciences) followed by quantification using the Empiria Studio Software package (LI-COR Biosciences). For each experiment, the optimum trypsin concentration for exclusively cleaving postsynaptic proteins was determined by comparing the extent of cleavage of pre- and postsynaptic marker proteins in the different samples. Results obtained at the optimum cleavage condition were used for the final quantification of the extent of cleavage of the tested proteins.

### **Postsynaptic density isolation**

The synaptosomal membrane fraction P3 was isolated as above except that entire mouse brains were homogenized with 12 strokes at 900 rpm and the homogenization buffer contained 320 mM sucrose, 20 mM HEPES, 5 mM EDTA, 1x cOmplete pH 7.4. The supernatant S2 containing soluble proteins was kept for immunoblotting analysis. The P3 pellet was resuspended in 1 ml of homogenization buffer, layered on top of a discontinuous sucrose cushion of 0.8, 1.0 and 1.2 M HEPES-buffered sucrose solution and centrifuged at 150000xg for 2 h. Following centrifugation, the synaptic plasma membrane fraction (SPM) at the interphase of 1.0 and 1.2 M sucrose was collected using an 18G needle on a 1 ml syringe. 2.5 volumes of 4 mM HEPES were added to the SPM to adjust the sucrose concentration from 1.2 M to 0.32 M. The SPM was then pelleted by centrifugation at 200,000xg for 30 min. The resulting pellet was resuspended in 300 µl of 50 mM HEPES buffer containing 2 mM EDTA and combined with 2.7 ml of 0.54% Triton X-100, 2 mM EDTA in 50 mM HEPES, followed by centrifugation at 32000xg for 20 min. The resulting PSD (postsynaptic density fraction) pellet was resuspended in 50 mM HEPES, 2 mM EDTA, pH 7.4. Protein concentration was measured by BCA assay. Equal protein amounts were diluted in 1x sample buffer and boiled at 95°C for 5 min. Samples were analyzed by immunoblotting.

### **Immunoprecipitation**

All steps were performed at 4°C in the presence of cOmplete™ EDTA-free protease inhibitor cocktail (Sigma-Aldrich). P2 (synaptosomal fraction) was prepared as described above and resuspended in lysis buffer (20 mM HEPES, 100 mM KCl, 1 mM MgCl<sub>2</sub>, 1 mM NaF, 1% sodium taurodeoxycholate (Sigma-Aldrich)). Protein concentration was measured by BCA assay. 4 mg of P2 lysate were incubated with 3 µg of primary antibody or with an equivalent amount of IgG control for 1 h on a rotating wheel prior to the addition of 25 µl Pierce™ Protein A/G Magnetic Beads (Thermo Fisher Scientific) for an additional 3 h. Following incubation, samples were washed 4x with lysis buffer, and proteins were eluted with 2x Laemmli sample buffer and analyzed by immunoblotting.

### **Pull-down assays**

GST-fusion proteins were expressed in *E.coli* (BL21) at 37°C for 4 h and coupled to glutathione-sepharose beads (Novagen) according to the manufacturer's instructions. Synaptosomal protein extract was prepared as described above. Protein concentration was measured by BCA assay. 50 µg of GST or GST-fusion protein were incubated with 3 mg of P2 lysate for 4 h under constant rotation at 4°C. Samples were washed 3x using lysis buffer, boiled with 2x Laemmli sample buffer and analyzed by immunoblotting.

### **SDS-PAGE and immunoblotting**

Samples were separated by SDS-PAGE using 4-12% Bis-Tris NuPage precast gels and 1x MOPS buffer. Proteins were transferred onto nitrocellulose membranes at 4°C in transfer buffer (15% methanol, 25 mM Tris base, 192 mM glycine) for 90 min at 110 V. Subsequently, membranes were washed twice with H<sub>2</sub>O, and transferred proteins were stained with Ponceau S solution (0.5% (w/v) Ponceau S, 1% (v/v) acetic acid) for 5 min. Background staining was removed by rinsing with 1% (v/v) acetic acid. Membranes were washed 2x 5 min with 0.1% (v/v) Tween-20 in tris-buffered saline (TBST), to remove residual Ponceau S, and were then incubated in Intercept<sup>R</sup> blocking buffer for 1 h at room temperature. Subsequently, membranes were incubated with primary antibodies (dilutions see antibody table S5) overnight at 4°C. Primary antibodies were diluted in 50% (v/v)

blocking buffer and 50% (v/v) TBST. Afterwards, membranes were washed 3x 5 min in TBST, and IRDye 800CW-conjugated secondary antibodies diluted 1:10,000 in TBST were applied for 1 h at room temperature. After washing 3x 5 min with TBST and 1x 5 min with TBS, signals were detected with the LI-COR Odyssey Fc Imaging system. Signals were analyzed, and images were exported using Image Studio. For re-probing, nitrocellulose membranes were incubated for 40 min in stripping buffer (25 mM glycine, 1% SDS, pH 2.25), washed 4x 10 min in TBST and subsequently blocked again for 1 h in Intercept<sup>R</sup> buffer before re-incubating with primary antibodies.

### **Statistical analysis**

Statistical data analysis was performed using the Graph Pad Prism 9 software. The specific tests used are stated in Table S6. Generally, unpaired two-tailed student's t-tests were used to compare two groups (genotypes). When data were not normally distributed, Mann-Whitney tests were used to compare two groups. When several groups were compared, generally one-way analysis of variance (ANOVA) tests were used followed by Holm-Sidak or Tukey's multiple comparison post-hoc tests to detect differences between experimental groups. When several groups were compared over time, two-way repeated-measures ANOVA tests were used followed by Holm-Sidak multiple comparison post-hoc tests. In case of fiber volley comparisons a mixed-effects model was used instead of a repeated-measures (RM) ANOVA, because some low-amplitude fiber volleys at small stimulation intensities could not be resolved and RM ANOVA requires no missing values. When paired not-normally distributed data was assessed for significant differences, a Friedman test with Dunn's multiple comparison post-hoc test was used comparing only against the control condition. The number of animals, slices, or cells is indicated in the figure legends and Table S6. In figures, significant differences are indicated by asterisks following this scheme: \*= $p < 0.05$ , \*\*= $p < 0.01$ , \*\*\*= $p < 0.001$ , \*\*\*\*= $p < 0.0001$ .  $p > 0.05$  is not significant and indicated as ns. Plotted data points in bar diagrams represent individual mice, individual slices, independent experiments etc. as specified by N in Table S6. Bars represent the arithmetic mean, error bars represent SEM (if not indicated otherwise in figure legends).

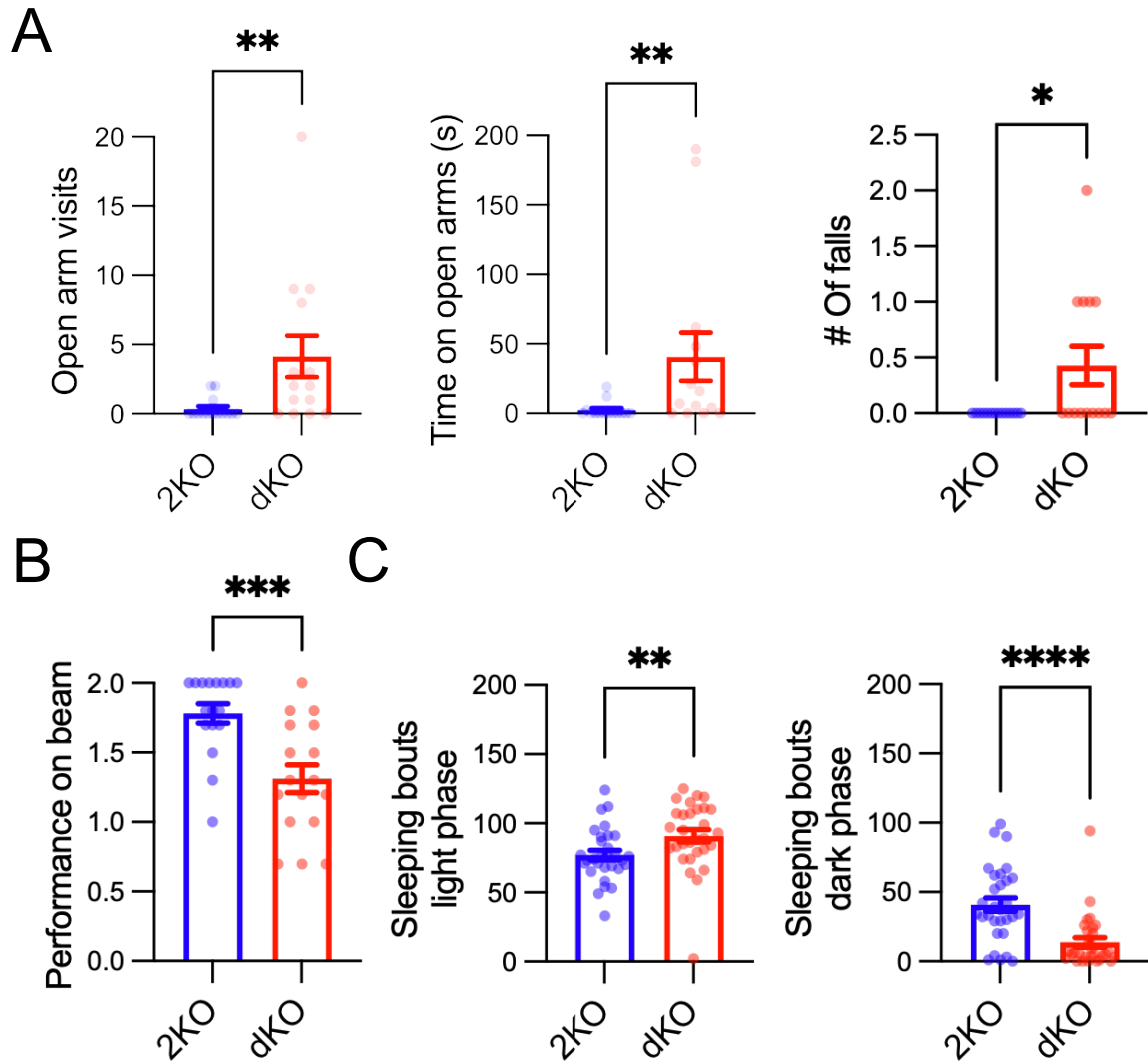


**Fig. S1. ITSN dKO mice exhibit alterations in anxiety-like behaviour, motor activity and sleep pattern**

**(A)** Intersectin dKO mice display reduced anxiety-like behaviour. Mice were placed for 5 min on an elevated plus maze. The number of open arm visits, the time spent on the open arms and the number of mice falling off the maze were significantly increased for the dKO mice (N=14 mice per genotype; Mann-Whitney test;  $*=p<0.05$ ,  $**=p<0.01$ ). **(B)** Intersectin dKO mice show reduced performance on a balance beam. Mice were placed in the middle of the beam. Performance was scored with "2" if the mice reached the adjacent cage on either side, with "1" if they fell off the beam after some time and with "0" if they fell immediately after placement (N=17 mice per genotype; Mann-Whitney test;  $***=p<0.001$ ). **(C)** Intersectin dKO mice have an altered sleeping pattern with more sleeping bouts during the light phase and less during the dark phase (N=30 mice per genotype; Mann-Whitney test;  $**=p<0.01$ ,  $****=p<0.0001$ ).

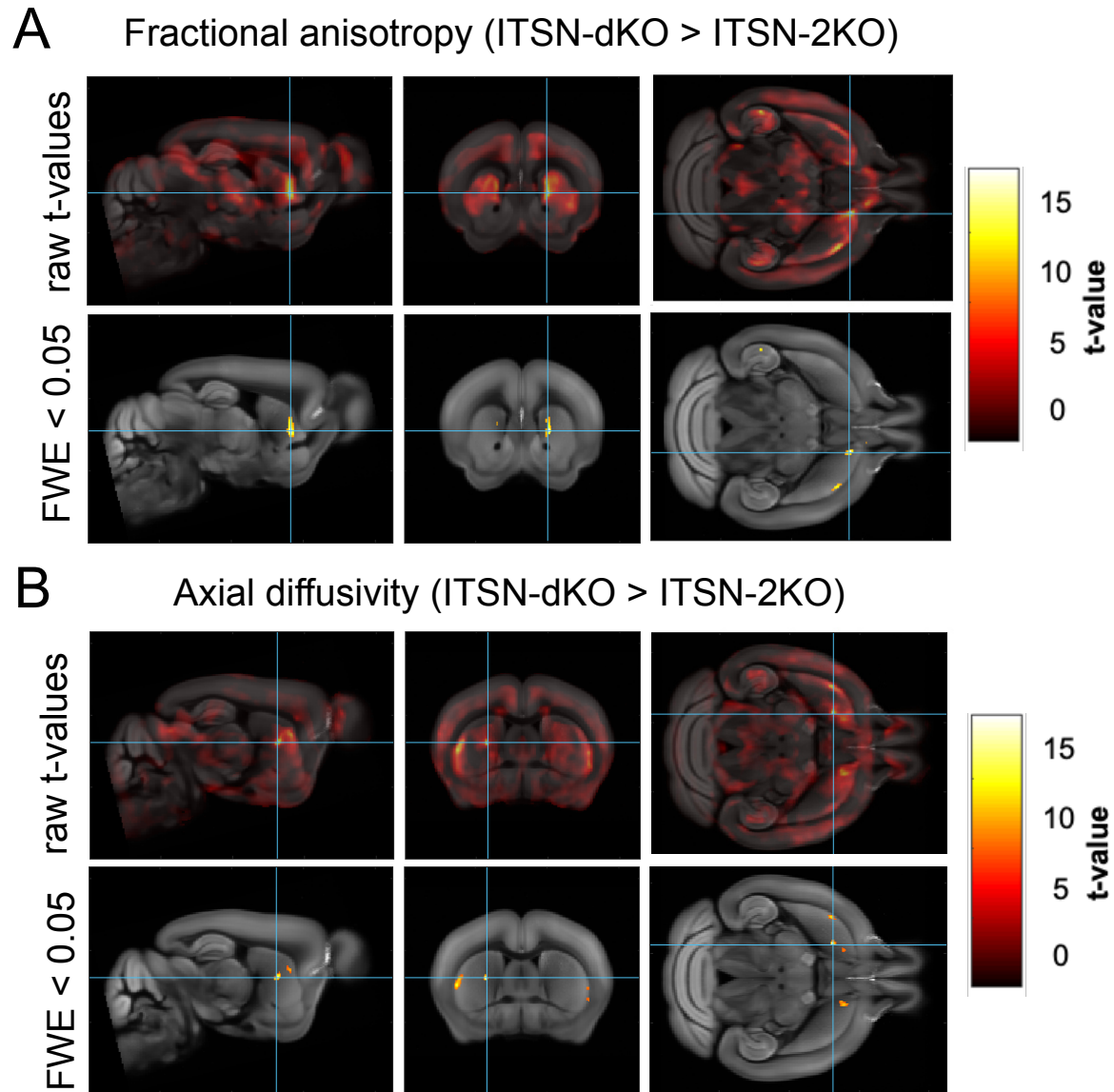


**Fig. S2. ITSN dKO brains exhibit changes in fractional anisotropy and axial diffusivity**

ITSN dKO mice show evidence for microstructural changes in the striatum, reflected by increased fractional anisotropy (A) and increased axial diffusivity (B). Changes of diffusion tensor imaging (DTI) parameters (2KO vs dKO) are color-coded and depicted as raw t-values (top panel) and also after family-wise error correction (bottom panel). Detailed values of voxel-wise DTI parameter changes are listed in Tables S3 and S4.

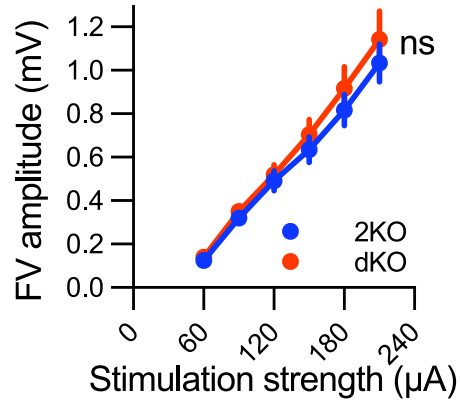


**Fig. S3. Fiber volley amplitudes are unchanged in ITSN dKO striatum**

Fiber volley amplitudes are not changed in ITSN dKO striatum indicating a comparable recruitment of presynaptic fibers (2KO: 22 slices from 5 animals, dKO: 21 slices from 5 animals; mixed-effects model; genotype effect:  $p=0.4762$ ).

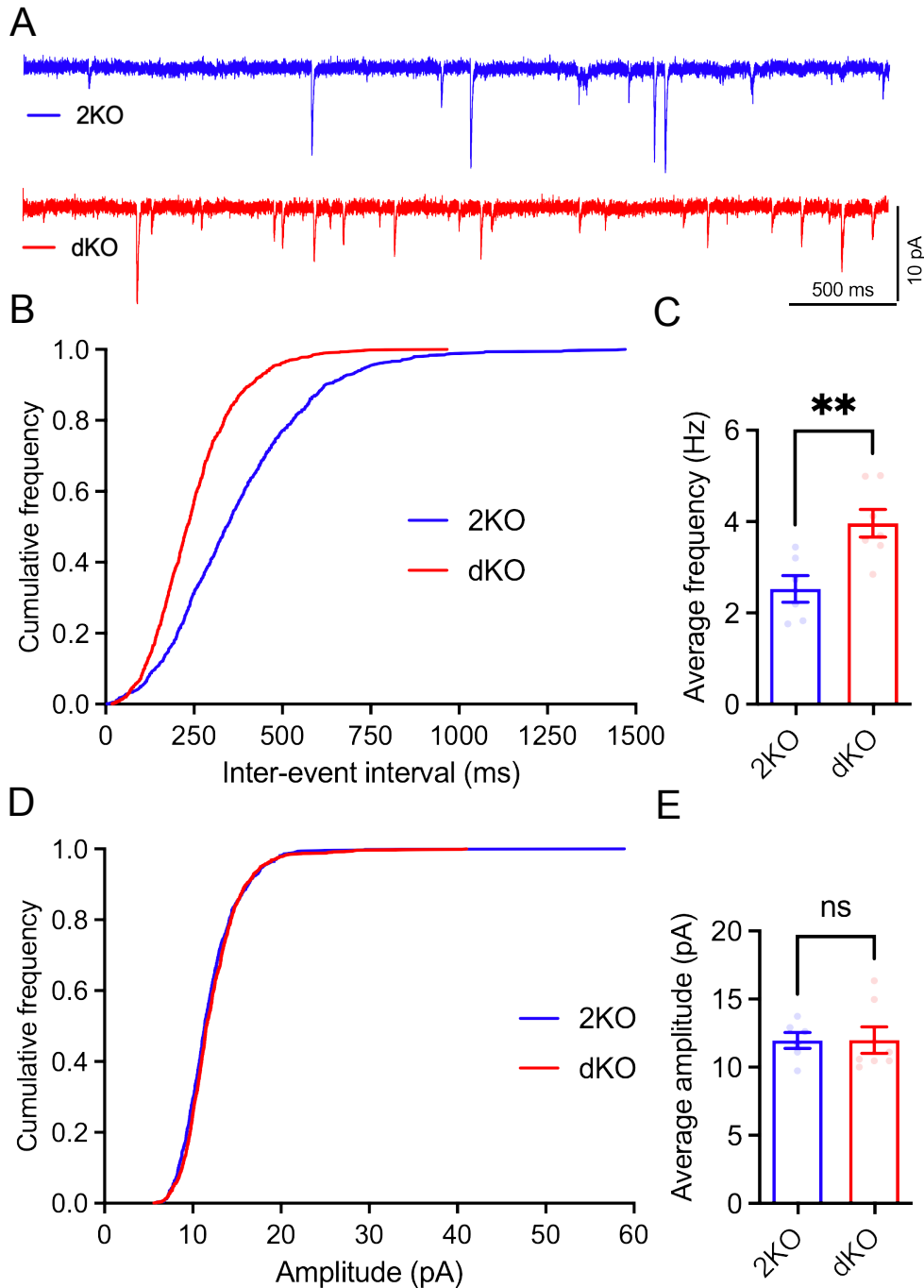


**Fig. S4. Enhanced spontaneous synaptic transmission upon loss of ITSN1/2**

(A-E) ITSN dKO neurons display an enhanced frequency of spontaneous excitatory synaptic transmission events, while amplitudes are unaltered. (A) Representative images of sEPSCs (spontaneous excitatory postsynaptic currents) recorded in the presence of 20  $\mu$ M Bicuculline and 50  $\mu$ M AP-5 to block inhibitory and NMDAR-mediated signaling. (B) Cumulative frequency distribution of inter-event intervals. (C) Average sEPSC frequency (ITSN 2KO: 6 cells from 3 animals, ITSN dKO: 7 cells from 3 animals; Mann-Whitney-Test; \*\*= $p < 0.01$ ). (D) Cumulative frequency distribution of sEPSC amplitudes. (E) Average sEPSC amplitude (ITSN 2KO: 6 cells from 3 animals, ITSN dKO: 7 cells from 3 animals; Mann-Whitney-Test; ns=non-significant). See statistics table S6 for additional details.

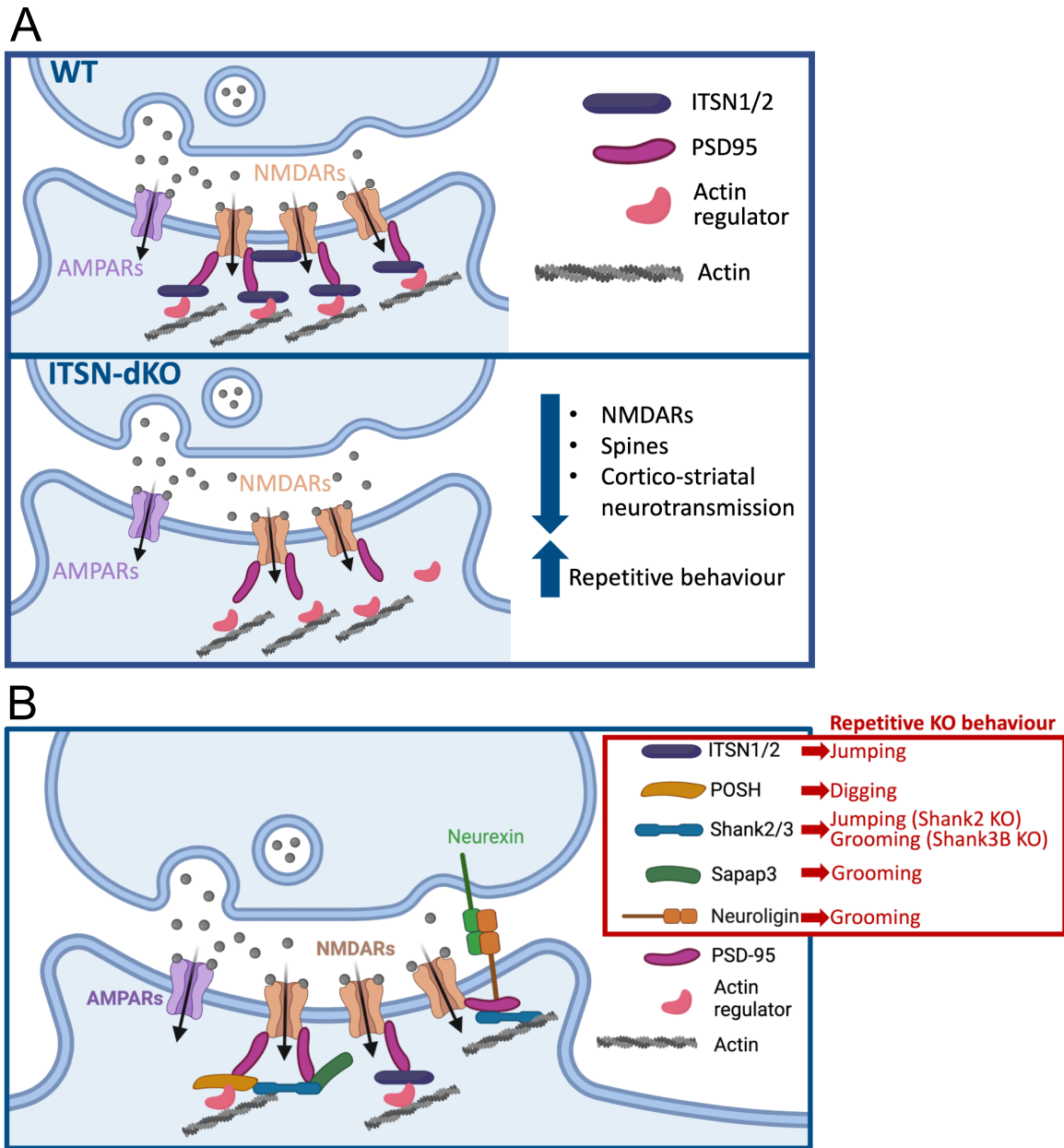


**Fig. S5. Scheme of postsynaptic intersectin loss-of-function phenotypes**

(A) Intersectins are part of a scaffolding complex that stabilizes NMDARs at the postsynaptic membrane. In absence of intersectins NMDARs, PSD95 and actin are partially lost from the postsynaptic membrane causing a decreased NMDAR/AMPA current ratio. Together with the observed reductions in spine numbers and cortico-striatal neurotransmission, these alterations might underlie the increase in repetitive behavior of ITSN dKO mice. (B) ITSN1/2 extend the repertoire of postsynaptic NMDAR interactors and scaffolds whose loss in mice causes repetitive behaviours. The type of repetitive behaviour caused by loss of ITSN1/2 (this paper), POSH (5), Shank2 (6), Shank3B (7), Sapap3 (8) and neuroligin (9) is stated in the red box.

**Table S1. Absolute regional brain volumes from MRI measurements**

Structure	Region	Sub-region	2KO	dKO	% Change dKO vs 2KO	p-value	significance level
Striatum			38.52 ±2.79	30.08 ±2.31	-21.91	0.000135	***
	dSTR	CPu	23.43 ±1.75	17.45 ±1.52	-25.53	0.000051	****
	vSTR		8.54 ±0.61	7.03 ±0.57	-17.65	0.001027	**
	sAMY		3.31 ±0.28	2.81 ±0.23	-15.13	0.006733	**
	LSX		3.5 ±0.31	3.02 ±0.17	-13.85	0.006008	**
Thalamus			19.37 ±1.21	15.16 ±0.87	-21.75	0.000036	****
	pmTH		11.13 ±0.78	8.62 ±0.53	-22.59	0.000043	****
	smTH		5.91 ±0.28	4.65 ±0.35	-21.38	0.000036	****
Pallidum			8.34 ±0.68	6.57 ±0.38	-21.14	0.000158	***
	dPAL		1.84 ±0.14	1.32 ±0.09	-28.44	0.000011	****
		GPi	0.34 ±0.04	0.23 ±0.03	-33.98	0.000135	***
		GPe	1.50 ±0.11	1.09 ±0.08	-27.18	0.000030	****
	mPAL		1.96 ±0.19	1.55 ±0.11	-20.93	0.000986	***
	cPAL		1.42 ±0.12	1.16 ±0.10	-18.60	0.001397	**
	vPAL		3.11 ±0.37	2.55 ±0.22	-18.11	0.008206	**
Hypothalamus			11.85 ±0.93	9.69 ±0.52	-18.21	0.000431	***
Olfactory areas			36.20 ±3.64	29.88 ±2.41	-17.45	0.004656	**
Midbrain			21.88 ±1.66	18.92 ±0.98	-13.53	0.003208	**
Medulla			31.63 ±2.83	27.91 ±1.72	-11.79	0.019883	*
Cortical subplate			6.11 ±0.49	5.42 ±0.59	-11.28	0.054082	ns
Isocortex			105.49 ±5.75	96.83 ±6.86	-8.21	0.041557	*
Hippocampal formation			36.78 ±2.25	33.94 ±3.04	-7.71	0.102683	ns
Pons			17.42 ±2.00	16.25 ±0.98	-6.73	0.256453	ns
Cerebellum			49.8 ±3.58	47.41 ±2.89	-4.8	0.263054	ns

Average absolute regional brain volumes (expressed in mm<sup>3</sup>) of ITSN 2KO and dKO mice. Values are given as arithmetic mean ± standard deviation (N = 9 animals per genotype; unpaired two-tailed t-test and adjusted for multiple comparisons using the Benjamini-Hochberg approach; \*=p<0.05, \*\*=p<0.01, \*\*\*=p<0.001, \*\*\*\*=p<0.0001, ns: not significant). For regional brain volumes expressed in % of total brain see Table S2. dSTR, dorsal striatum = CPu, caudate putamen; vSTR, ventral striatum; sAMY, striatum-like amygdalar nuclei; LSX, lateral septal complex; pmTH, polymodal association cortex-related thalamus; smTH, sensorimotor cortex-related thalamus; dPAL, dorsal

pallidum; GPi, globus pallidus internal part; GPe, globus pallidus external part; mPAL, medial pallidum; cPAL, caudal pallidum; vPAL, ventral pallidum.

**Table S2. Normalized regional brain volumes from MRI measurements**

Structure	Region	Sub-region	2KO	dKO	% Change dKO vs 2KO	p-value	significance level
Striatum			8.18 ±0.07	7.23 ±0.15	-11.61	0.00000001	****
	dSTR	CPu	4.98 ±0.07	4.19 ±0.14	-15.73	0.00000002	****
	vSTR		1.82 ±0.06	1.69 ±0.06	-6.84	0.01092520	*
	sAMY		0.70 ±0.02	0.68 ±0.04	-3.81	0.26945692	ns
	LSX		0.74 ±0.04	0.73 ±0.03	-2.33	0.51864729	ns
Thalamus			4.12 ±0.11	3.65 ±0.09	-11.41	0.00000296	****
	pmTH		2.37 ±0.09	2.07 ±0.07	-12.35	0.00004966	****
	smTH		1.26 ±0.05	1.12 ±0.05	-11.11	0.00103618	**
Pallidum			1.77 ±0.03	1.58 ±0.04	-10.59	0.00000278	****
	dPAL		0.39 ±0.01	0.32 ±0.02	-18.84	0.00000204	****
		GPI	0.07 ±0.01	0.05 ±0.01	-24.94	0.00240660	**
		GPe	0.32 ±0.01	0.26 ±0.02	-17.45	0.00002015	****
	mPAL		0.42 ±0.02	0.37 ±0.03	-10.21	0.01402982	*
	cPAL		0.30 ±0.03	0.28 ±0.02	-7.98	0.15850622	ns
	vPAL		0.66 ±0.05	0.61 ±0.03	-7.13	0.12914767	ns
Hypothalamus			2.52 ±0.07	2.33 ±0.09	-7.27	0.00437708	**
Olfactory areas			7.68 ±0.32	7.19 ±0.25	-6.41	0.02473205	*
Midbrain			4.65 ±0.11	4.56 ±0.13	-1.98	0.35265499	ns
Medulla			6.72 ±0.43	6.73 ±0.47	0.1	0.98427590	ns
Cortical subplate			1.30 ±0.05	1.30 ±0.07	0.3	0.95076966	ns
Isocortex			22.44 ±0.53	23.29 ±0.47	3.8	0.02614881	*
Hippocampal formation			7.82 ±0.28	8.16 ±0.35	4.31	0.15638125	ns
Pons			3.69 ±0.22	3.91 ±0.17	5.95	0.14348068	ns
Cerebellum			10.58 ±0.28	11.41 ±0.29	7.83	0.00085419	***

Average normalized regional brain volumes (expressed as % of total brain) of ITSN 2KO and dKO mice. Values are given as arithmetic mean  $\pm$  standard deviation (N=9 animals per genotype; unpaired two-tailed t-test and adjusted for multiple comparisons using the Benjamini-Hochberg approach; \*= $p < 0.05$ , \*\*= $p < 0.01$ , \*\*\*= $p < 0.001$ , \*\*\*\*= $p < 0.0001$ , ns: not significant). dSTR, dorsal striatum = CPu, caudate putamen; vSTR, ventral striatum; sAMY, striatum-like amygdalar nuclei; LSX, lateral septal complex; pmTH, polymodal association cortex-related thalamus; smTH, sensorimotor cortex-related thalamus; dPAL, dorsal pallidum; GPI, globus pallidus internal part;

GPe, globus pallidus external part; mPAL, medial pallidum; cPAL, caudal pallidum; vPAL, ventral pallidum.

**Table S3. Fractional anisotropy changes in ITSN dKO striatum**

Region	Cluster size k	peak p-value	peak t-value	Coordinates		
				x mm	y mm	z mm
Caudoputamen	154	0.00012	16.44	1.25	1.01	-3.06
Caudoputamen	138	0.00073	14.30	3.21	0.31	-3.41
Caudoputamen	138	0.00130	13.66	3.00	0.38	-2.92
Field CA1, pyramidal layer	25	0.00095	14.02	-3.86	-3.40	-3.13
Anterior olfactory nucleus, medial part	21	0.0036	12.65	0.83	1.85	-3.20
Main olfactory bulb, granule layer	8	0.0087	11.64	1.46	3.46	-1.24
Field CA1, stratum radiatum	92	0.0089	11.61	-3.23	-3.40	-2.15
Field CA1, stratum radiatum	92	0.0093	11.56	-2.74	-3.47	-1.73
Caudoputamen	11	0.013	11.18	-1.20	0.94	-2.85
Field CA1, pyramidal layer	8	0.019	10.74	3.77	-3.54	-2.85
Field CA1, pyramidal layer	13	0.025	10.44	-4.00	-3.47	-3.69
Field CA3, stratum radiatum	5	0.026	10.39	3.00	-3.19	-3.83
Field CA1, stratum lacunosum-moleculare	3	0.028	10.30	3.07	-2.98	-4.25
Main olfactory bulb	4	0.029	10.27	-1.20	3.88	-1.59
Caudoputamen	4	0.04	9.91	1.53	0.87	-2.36

Voxel-wise statistics of fractional anisotropy (FA) maps. Data were smoothed using an isotropic gaussian filter kernel with full width at half maximum (FWHM) of 0.28 mm, and significant results (dKO > 2KO) were reported using family-wise error (FWE) correction at  $p < 0.05$  and a cluster size of  $k=1$ . Significant voxels located in striatal brain structures are highlighted in blue. All coordinates refer to the Allen brain space and represent peaks of surviving clusters.

**Table S4. Axial diffusivity changes in ITSN dKO striatum**

Region	Cluster size k	peak p-value	peak t-value	Coordinates		
				x mm	y mm	z mm
Caudoputamen	47	0.000011	19.63	-1.69	0.31	-2.85
Nucleus accumbens	272	0.000029	18.23	1.18	1.01	-3.20
Caudoputamen	202	0.00030	15.30	-3.16	0.31	-3.20
Superior colliculus, motor related, intermediate gray layer, sublayer b	34	0.00041	14.93	-0.08	-3.40	-2.15
Caudoputamen	85	0.0019	13.31	-2.74	0.73	-3.76
Supplemental somatosensory area, layer 2/3	3	0.0036	12.65	-4.14	-0.32	-1.94
Caudoputamen	69	0.0054	12.22	-1.27	0.66	-3.27
Field CA1, stratum radiatum	12	0.0056	12.20	-3.79	-3.40	-3.13
Caudoputamen	45	0.0057	12.17	-1.62	0.94	-2.43
Caudoputamen	45	0.0064	12.03	3.21	0.38	-3.90
Caudoputamen	45	0.0170	10.89	3.28	0.24	-3.34
Main olfactory bulb, granule layer	16	0.0081	11.75	1.46	3.39	-1.31
Superior colliculus, motor related, intermediate gray layer, sublayer a	11	0.012	11.28	1.53	-4.03	-2.01
Basic cell groups and regions	10	0.014	11.06	-1.13	3.60	-2.08
Anterior olfactory nucleus, medial part	5	0.020	10.72	0.76	1.85	-3.13
Basic cell groups and regions	6	0.023	10.53	-1.13	3.67	-1.52
Caudoputamen	11	0.024	10.50	-2.25	1.01	-3.55
Main olfactory bulb, granule layer	3	0.029	10.27	-1.55	3.39	-1.45
Basic cell groups and regions	11	0.036	10.05	1.18	3.67	-1.59
Basomedial amygdalar nucleus, posterior part	1	0.043	9.85	-2.81	-1.44	-5.51

Voxel-wise statistics of axial diffusivity (AD) maps. Data were smoothed using an isotropic gaussian filter kernel with full width at half maximum (FWHM) of 0.28 mm, and significant results (dKO > 2KO) were reported using family-wise error (FWE) correction at  $p < 0.05$  and a cluster size of  $k=1$ . Significant voxels located in striatal brain structures are highlighted in blue. All coordinates refer to the Allen brain space and represent peaks of surviving clusters.

**Table S5. Antibodies**

Antigen	Species	Dilution WB	Dilution IF	Amount IP	Supplier / #
Actin	mouse	1:10000	--	--	Sigma Aldrich #A5441
Bassoon	guineapig	--	1:500	--	Synaptic Systems #141004
GluA1	mouse	1:1000	--	--	Merck Millipore #MAB2263
GluA2	mouse	1:1000	--	--	Merck Millipore #MAB397
Homer 1	mouse	1:500	1:500	--	Synaptic Systems #160011
ITSN1	rabbit	1:1000	1:200	--	homebrew #475 (mSH3A-C)
ITSN1	rabbit	--	--	3 $\mu$ g	homebrew #476 (1-440)
ITSN1	mouse	1:200	--	--	Santa Cruz #sc-136242
Munc18-1	rabbit	1:1000	--	--	Synaptic Systems #116002
NR1	mouse	1:1000	--	--	Synaptic Systems #114011
NR2A	rabbit	1:500	--	--	Merck Millipore #07-632
NR2B	rabbit	1:1000	--	--	Merck Millipore #06-600
Pre-immune serum	rabbit	--	--	3 $\mu$ g	homebrew
PSD95	mouse	1:1000	--	--	Synaptic Systems #124011
Rab3a	mouse	1:4000	--	--	Synaptic Systems #107111
SNAP25	mouse	1:500	--	--	Synaptic Systems #111011
Synaptophysin1	mouse	1:4000	--	--	Synaptic Systems #101011
Synaptophysin1	mouse	1:500	--	--	Synaptic Systems #101011C3
Tubulin, b3	rabbit	1:8000	--	--	Synaptic Systems #302302

**Table S6. Statistical Data**

Figure	Data type	Sample size (N) and p value	Statistical test
<b>10 min mouse observation in home cage environment &amp; nesting experiment</b>			
1A Corner jumps	mean±SEM ITSN-dKO: 121.6±42.31 ITSN-2KO: 0±0	N(ITSN-dKO) = 19 mice N(ITSN-2KO) = 22 mice p<0.0001 (****)	Mann-Whitney test (Prism 9)
1B Upright running	mean±SEM ITSN-dKO: 1.579±0.6367 ITSN-2KO: 0±0	N(ITSN-dKO) = 19 mice N(ITSN-2KO) = 22 mice p=0.0008 (***)	Mann-Whitney test (Prism 9)
1C Abrupt movements	mean±SEM ITSN-dKO: 5.368±1.886 ITSN-2KO: 1.045±0.6916	N(ITSN-dKO) = 19 mice N(ITSN-2KO) = 22 mice p=0.0081 (**)	Mann-Whitney test (Prism 9)
1D Wall rearings	mean±SEM ITSN-dKO: 25.32±4.304 ITSN-2KO: 33.32±2.832	N(ITSN-dKO) = 19 mice N(ITSN-2KO) = 22 mice p=0.1194 (ns)	Unpaired two-tailed t-test
1E Grooming episodes	mean±SEM ITSN-dKO: 1.947±0.2226 ITSN-2KO: 2.773±0.4105	N(ITSN-dKO) = 19 mice N(ITSN-2KO) = 22 mice p=0.1925 (ns)	Mann-Whitney test (Prism 9)
1F Marbles moved	mean±SEM ITSN-dKO: 0.3333±0.2108 ITSN-2KO: 13.00±2.113	N(ITSN-dKO) = 6 mice N(ITSN-2KO) = 6 mice p=0.0022 (**)	Mann-Whitney test (Prism 9)
1F Marble coverage (%)	mean±SEM ITSN-dKO: 0.023±0.023 ITSN-2KO: 25.85±6.988	N(ITSN-dKO) = 6 mice N(ITSN-2KO) = 6 mice p=0.0022 (**)	Mann-Whitney test (Prism 9)
1G Interactions with paper	mean±SEM ITSN-dKO: 3.263±1.372 ITSN-2KO: 12.64±1.524	N(ITSN-dKO) = 19 mice N(ITSN-2KO) = 22 mice p<0.0001 (****)	Unpaired two-tailed t-test
1H Nest score	mean±SEM ITSN-dKO: 0.1765±0.1282 ITSN-2KO: 2.105±0.2405	N(ITSN-dKO) = 17 mice N(ITSN-2KO) = 19 mice p<0.0001 (****)	Mann-Whitney test (Prism 9)
<b>24 h mouse observation in activity meter &amp; fluoxetine treatment</b>			
1I Time spent in periphery	mean±SEM ITSN-dKO: 20.02±0.2605 ITSN-2KO: 18.19±0.5221	N(ITSN-dKO) = 30 mice N(ITSN-2KO) = 30 mice p<0.0063 (**)	Mann-Whitney test (Prism 9)
1J Corner jumps	mean±SEM ITSN-dKO: 58982±12356 ITSN-2KO: 2237±259.5	N(ITSN-dKO) = 30 mice N(ITSN-2KO) = 30 mice p<0.0003 (***)	Mann-Whitney test (Prism 9)
1K Distance travelled	mean±SEM ITSN-dKO: 7023±301.6 ITSN-2KO: 5442±231.4	N(ITSN-dKO) = 30 mice N(ITSN-2KO) = 30 mice p=0.0001 (***)	Unpaired two-tailed t-test
1L Locomotion Speed	mean±SEM ITSN-dKO: 12.3±0.5553 ITSN-2KO: 10.1±0.3535	N(ITSN-dKO) = 30 mice N(ITSN-2KO) = 30 mice p=0.0047 (**)	Mann-Whitney test (Prism 9)

1M Fluoxetine	mean±SEM ITSN-dKO pre FX: 108793±20177 ITSN-dKO FX: 31373±14823 ITSN-dKO post: 81554±22720	N(ITSN-dKO) = 6 mice pre FX vs. FX: p=0.0078 (**) pre vs. post FX: p>0.9999 (ns)	Friedman test with Dunn's multiple comparison test against "pre" as control column (Prism 9)
<b>Analysis of brain volume (For 2C see tables S1 and S2)</b>			
2A Brain volume	mean±SEM ITSN-2KO: 470.476±10.1975 ITSN-dKO: 415.476±8.08267	N(ITSN-dKO)=9 mice N(ITSN-2KO)=9 mice p=0.0006 (***)	Unpaired two- tailed t-test
<b>Morphology of medium spiny neurons; analysis of basal transmission; analysis of AMPA/NMDA receptor currents and plasticity</b>			
3B Sholl intersections	Genotype main effect F (1, 12) = 8.449	N(ITSN-dKO): 7 cells from at least 3 mice N(ITSN-2KO): 7 cells from at least 3 mice Genotype effect: p=0.0132 (*)	Two-way RM ANOVA
3C Sholl AUC	mean±SEM ITSN-2KO: 3161±231.7 ITSN-dKO: 2253±204.8	N(ITSN-dKO): 7 cells from at least 3 mice N(ITSN-2KO): 7 cells from at least 3 mice p=0.0124 (*)	Unpaired two- tailed t-test
3E Spine density	mean±SEM ITSN-2KO: 1.154±0.05603 ITSN-dKO: 0.6522±0.04976	N(ITSN-dKO): 7 cells from at least 3 mice N(ITSN-2KO): 7 cells from at least 3 mice p<0.0001 (****)	Unpaired two- tailed t-test
3G Population spike amplitude	Genotype main effect F (1, 41) = 12.73	N(ITSN-dKO): 21 slices from 5 mice N(ITSN-2KO): 22 slices from 5 mice Genotype effect: p=0.0009 (***)	Two-way RM ANOVA followed by Holm-Sidak multiple comparison test
S3A Fiber volley amplitude	Genotype fixed effect F (1, 41) = 0.5170	N(ITSN-dKO): 21 slices from 5 mice N(ITSN-2KO): 22 slices from 5 mice Genotype effect: p=0.4762 (ns)	Mixed-effects model
3I NMDA/ AMPA ratio	mean±SEM ITSN-2KO: 0.4581±0.07482 ITSN-dKO: 0.2632±0.04289	N(ITSN-dKO): 11 cells from 4 mice N(ITSN-2KO): 10 cells from 4 mice p=0.0321 (*)	Unpaired two- tailed t-test
3J PS Amplitude (% baseline)	Genotype fixed effect F (1, 14) = 5.723	N(ITSN-dKO): 7 slices from 3 mice N(ITSN-2KO): 9 slices from 3 mice Genotype effect: p=0.0313 (*)	Two-way RM ANOVA
3K LTD (% baseline)	mean±SEM ITSN-2KO: 59.7±5.5% of baseline ITSN-dKO: 81.0±3.4% of baseline	N(ITSN-dKO): 7 slices from 3 mice N(ITSN-2KO): 9 slices from 3 mice p=0.0082 (**)	Unpaired two- tailed t-test

<b>Analysis of postsynaptic localization and synaptic protein levels</b>			
4A Protein cleavage (%)	mean±SEM GluA1: 9.333±1.448 GluA2: 13.58±2.103 SYP: 84.67±6.717 SNAP25: 84.33±11.49 ITSN1: 41.17±7.034	N(GluA1, GluA2)=3 N(SYP, SNAP25, ITSN1)=4 GluA1 vs SYP: p=0.0001 GluA1 vs SNAP25: p=0.0001 GluA2 vs SYP: p=0.0002 GluA2 vs SNAP25: p=0.0002 SYP vs ITSN1: p=0.0073 SNAP25 vs ITSN1: p=0.0078	One-way ANOVA with Tukey's post test
4G WB	mean±SEM Tubulin: 1.0±0.047 (2KO), 0.928±0.074 (dKO) GluA2: 1.0±0.045 (2KO), 1.019±0.040 (dKO) GluA1: 1.0±0.044 (2KO), 1.002±0.067 (dKO) Actin: 1.0±0.040 (2KO), 0.802±0.015 (dKO) PSD95: 1.0±0.032 (2KO), 0.800±0.037 (dKO) NR2B: 1.0±0.048(2KO), 0.839±0.042 (dKO) NR2A: 1.0±0.019 (2KO), 0.612±0.018 (dKO) ITSN1: 1.0±0.080 (2KO), 0.088±0.024 (dKO)	N(ITSN-dKO): lysates from 4 mice N(ITSN-2KO): lysates from 4 mice Tubulin: p=0.446496 (ns) GluA2: p=0.760295 (ns) GluA1: p=0.979845 (ns) Actin: p=0.003634 (**) PSD95: p=0.006571 (**) NR2B: p=0.045562 (*) NR2A: p=0.000006 (****) ITSN1: p=0.000034(****)	Unpaired two-tailed t-test
<b>Analysis of behavioral experiments displayed in supplementary figure 1</b>			
S1A EPM Open arm visits	mean±SEM ITSN-2KO: 0.3571±0.1991 ITSN-dKO: 4.143±1.508	N(ITSN-2KO)=14 mice N(ITSN-dKO)=14 mice p=0.0042 (**)	Mann-Whitney test (Prism 9)
S1A EPM Time on open arms	mean±SEM ITSN-2KO: 2.386±1.539 ITSN-dKO: 40.83±17.20	N(ITSN-2KO)=14 mice N(ITSN-dKO)=14 mice p=0.0037 (**)	Mann-Whitney test (Prism 9)
S1A EPM # of falls	mean±SEM ITSN-2KO: 0.000±0.000 ITSN-dKO: 0.4286±0.1727	N(ITSN-2KO)=14 mice N(ITSN-dKO)=14 mice p=0.0407 (*)	Mann-Whitney test (Prism 9)
S1B Performance on beam	mean±SEM ITSN-2KO: 1.782±0.06979 ITSN-dKO: 1.312±0.09922	N(ITSN-2KO)=17 mice N(ITSN-dKO)=17 mice p=0.0005 (****)	Mann-Whitney test (Prism 9)
S1C Sleeping bouts light phase	mean±SEM ITSN-2KO: 77±3.509 ITSN-dKO: 90.93±4.479	N(ITSN-2KO)=30 mice N(ITSN-dKO)=30 mice p=0.0031 (**)	Mann-Whitney test (Prism 9)
S1C Sleeping bouts dark phase	mean±SEM ITSN-2KO: 40.93±4.918 ITSN-dKO: 13.73±3.478	N(ITSN-2KO)=30 mice N(ITSN-dKO)=30 mice p<0.0001 (****)	Mann-Whitney test (Prism 9)

<b>Analysis of spontaneous neurotransmission displayed in supplementary figure 4</b>			
S4C average frequency	mean±SEM ITSN-2KO: 2.528±0.2905 ITSN-dKO: 3.963±0.3035	N(ITSN-2KO)=6 cells from 3 animals N(ITSN-dKO)=7 cells from 3 animals p=0.0047 (**)	Mann-Whitney test (Prism 9)
S4E average amplitude	mean±SEM ITSN-2KO: 11.97±0.5830 ITSN-dKO: 12.00±0.9680	N(ITSN-2KO)=6 cells from 3 animals N(ITSN-dKO)=7 cells from 3 animals p=0.7308 (ns)	Mann-Whitney test (Prism 9)

## Movie S1 (separate file)

Legend to Movie S1:

### **Obsessive corner jumping by ITSN dKO mice**

Excerpt from a 10 min observation of an ITSN dKO mouse in its home cage environment demonstrating stereotypic and repetitive corner jumping.

### **SI References**

1. Y. Yu *et al.*, Mice deficient for the chromosome 21 ortholog *Itsn1* exhibit vesicle-trafficking abnormalities. *Hum Mol Genet* **17**, 3281-3290 (2008).
2. F. Gerth *et al.*, Intersectin associates with synapsin and regulates its nanoscale localization and function. *Proc Natl Acad Sci U S A* **114**, 12057-12062 (2017).
3. A. I. Pack *et al.*, Novel method for high-throughput phenotyping of sleep in mice. *Physiol Genomics* **28**, 232-238 (2007).
4. S. Koch *et al.*, Atlas registration for edema-corrected MRI lesion volume in mouse stroke models. *J Cereb Blood Flow Metab* **39**, 313-323 (2019).
5. M. Yao *et al.*, POSH regulates assembly of the NMDAR/PSD-95/Shank complex and synaptic function. *Cell Rep* **39**, 110642 (2022).
6. H. Won *et al.*, Autistic-like social behaviour in Shank2-mutant mice improved by restoring NMDA receptor function. *Nature* **486**, 261-265 (2012).
7. J. Peca *et al.*, Shank3 mutant mice display autistic-like behaviours and striatal dysfunction. *Nature* **472**, 437-442 (2011).
8. J. M. Welch *et al.*, Cortico-striatal synaptic defects and OCD-like behaviours in Sapap3-mutant mice. *Nature* **448**, 894-900 (2007).
9. J. Blundell *et al.*, Neuroligin-1 deletion results in impaired spatial memory and increased repetitive behavior. *J Neurosci* **30**, 2115-2129 (2010).